

# HiFT: A Hierarchical Full Parameter Fine-Tuning Strategy

Yongkang Liu<sup>1,2,4</sup>, Yiqun Zhang<sup>1</sup>, Qian Li<sup>3</sup>, Tong Liu<sup>2,4</sup>,  
Shi Feng<sup>1</sup>, Daling Wang<sup>1</sup>, Yifei Zhang<sup>1</sup> and Hinrich Schütze<sup>2,4</sup>

<sup>1</sup>Northeastern University, China

<sup>2</sup>CIS, LMU Munich, Germany

<sup>3</sup>SHANDONG University, China

<sup>4</sup>Munich Center for Machine Learning (MCML), Germany

misonksy@163.com, yiqunzhang@stumail.neu.edu.cn, TongLiu.physics@gmail.com  
feiwangyuzhou@sdu.edu.cn, {fengshi, wangdaling, zhangyifei}@cse.neu.edu.cn

## Abstract

Full-parameter fine-tuning (FPFT) has become the go-to choice for adapting language models (LMs) to downstream tasks due to its excellent performance. As LMs grow in size, fine-tuning the full parameters of LMs requires a prohibitively large amount of GPU memory. Existing approaches utilize zeroth-order optimizer to conserve GPU memory, which potentially compromises the performance of LMs as non-zero order optimizers tend to converge more readily on most downstream tasks. In this paper, we propose a novel optimizer-independent end-to-end hierarchical fine-tuning strategy, HiFT, which only updates a subset of parameters at each training step. HiFT significantly reduces the amount of gradients and optimizer state parameters residing in GPU memory at the same time, thereby reducing GPU memory usage. Our results demonstrate that: (1) HiFT achieves comparable performance with parameter-efficient fine-tuning and standard FPFT. (2) Results on six models show that HiFT reduces the number of trainable parameters by about 89.18% on average compared to FPFT. (3) HiFT supports FPFT of 7B models for 24G GPU memory devices under mixed precision without using any memory saving techniques. (4) HiFT supports various optimizers including AdamW, AdaGrad, SGD, etc.

## 1 Introduction

Full-Parameter Fine-Tuning (FPFT) Language Models (LMs) has been a successful paradigm in various downstream tasks (Vaswani et al., 2017; Lewis et al., 2020; Liu et al., 2020; Lv et al., 2023). However, as the size of LMs becomes larger, FPFT LMs requires immense memory, which has become an obstacle to conduct research.

One line of research to reduce memory is to use heterogeneous memory (Pudipeddi et al., 2020; Rajbhandari et al., 2021) (e.g., GPU, CPU, and NVMe memory) or distributed techniques (e.g., tensor parallelism (Shazeer et al., 2018; Shoeybi et al., 2019;

Zhang et al.; Kim et al., 2023; Wu et al., 2023)).

These strategies require parameter sharing across diverse devices and thus usually introduce a significant communication burden. Parameter-Efficient Fine-Tuning (PEFT) is another line of strategies for memory reduction, categorized into addition-based, selection-based, and reparametrization-based methods (Lialin et al., 2023). The addition-based methods (e.g., Prefix-Tuning (Li and Liang, 2021), AttentionFusion (Cao et al., 2022)) reduce the number of trainable parameters by only updating newly added parameters and freezing the weights of LMs. Although these methods reduce the number of parameters for fine-tuning, they expand the number of model parameters and increase the burden on forward propagation. The selection-based methods (e.g., BitFit (Zaken et al., 2022), LT-SFT (Ansell et al., 2022), FAR (Vucetic et al., 2022)), on the other hand, fine-tune a subset of model parameters, resulting in a performance gap with FPFT. The reparametrization-based methods (e.g., LoRA (Hu et al., 2022a), KronA (Edalati et al., 2022), S4-model (Chen et al., 2023)) leverage low-rank decomposition to minimize the number of trainable parameters. Using low-rank representations inevitably leads to information loss and performance degradation. PEFT involves a trade-off between serving efficiency and quality. According to existing works (Raschka, 2023; Artur et al., 2023; Kourosh and Rehaan, 2023), FPFT still maintains advantages in performance on most benchmarks.

Some works have reduced memory usage for FPFT by removing the momentum state of the optimizer. LOMO (Lv et al., 2023) reduces the memory usage of the optimizer momentum and gradients by integrating gradient calculation and update. However, LOMO requires forward propagation twice. In addition, LOMO forces the model to be 16-bit quantized and uses the gradient checkpointing technique (Chen et al., 2016) to reduce memory usage while LOMO has limited memory savings in real-

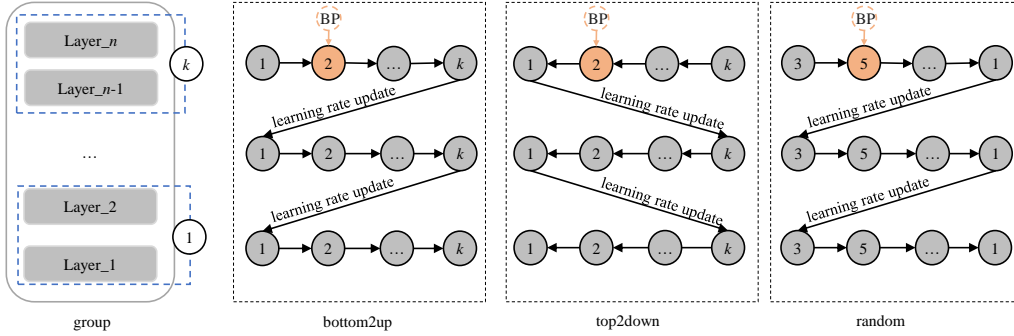


Figure 1: Schematic diagram of our HiFT. **group** represents the grouping operation of the layers. **bottom2up**, **top2down** and **random** are training strategies. Gray indicates that the corresponding parameters are in the frozen state, and brown indicates that the corresponding parameters are in the activated state.  $k$  is the number of groups,  $n$  is the number of layers of the given model, and BP denotes parameter update through back propagation.

world scenarios. MeZO (Malladi et al., 2023) designs a zeroth-order optimizer to reduce memory usage. However, MeZO is unstable and performs poorly without prompts. These methods make the momentum optimizers unusable, while the momentum optimizers such as AdamW (Loshchilov and Hutter, 2017) have been proven to be superior in improving the performance.

In order to perform FPFT on low-memory devices, we propose a novel end-to-end **H**ierarchical **F**ine-Tuning (**HiFT**) strategy, adopting the idea of layer-by-layer training. HiFT divides the layers of the model into different groups. At each training step, HiFT updates the parameters of one group while freezing the others. Compared to standard FPFT, HiFT leads to different groups of parameters being updated with different learning rates. This causes the model parameters to be updated in an inconsistent amplitude, which leads to a decrease in model performance. To solve this problem, we adopt to delay the learning rate update, which only updates the learning rate once when all layers of model are updated. HiFT is also different from layer-wise training (Bengio et al., 2006), where the layer-wise training incrementally adds new layers to a pre-trained shallow model, only updating the newly added parameters at each training stage until all layers are updated. As a result, layer-wise strategy produces accumulated errors at different training stages due to its pipeline training.

HiFT can significantly reduce the number of trainable parameters per training step. We only keep the momentum and gradients of the parameters that need to be updated on the GPU device due to only a portion of the parameters are updated at each training step. This helps to reduce the GPU memory usage of the optimizer states and gradients.

Assuming we divide the layers of the model into  $k$  groups, the average memory usage by gradients and optimizer states is then only  $1/k$  of standard FPFT theoretically. With the batch size being 1 and the sentence length being 512, using the HiFT strategy to full-parameter fine-tuning a 7B model requires about 16.87G, and a 13B model requires about 31G of memory. Given that the memory occupied by forward activations is also related to the input, we discuss the further details in experiments. Another important conclusion is HiFT does not significantly increase the time for fine-tuning. The main reason is that the amount of trainable parameters in a single step is reduced, the training speed of each step is accordingly improved. Although HiFT requires larger epochs (Under the same batch, generally 2 to 3 times and up to 5 times that of standard FPFT. With larger batches, the fine-tuning time gets greatly reduced.), due to the increase in the fine-tuning speed of a single step, the overall time does not increase significantly. In short, HiFT significantly saves the memory of FPFT at a slight time cost without losing performance.

## 2 Related Work

**Full-Parameter Fine-tuning** FPFT fine-tunes the pre-trained LMs on specific tasks by updating all parameters (Sun et al., 2023; Lin et al., 2024; Ma et al., 2024), which requires massive computing power as the parameters of LMs increase. Mixed-precision training enables high-throughput computations by employing half-precision storage for parameters, activations, and gradients (Rajbhandari et al., 2020a; Narayanan et al., 2021). Staged training incrementally increases the amount of compute and reuse the compute from prior stages (Shen et al., 2022). These methods increase the parameter

consumption when training precision or operators. LOMO (Lv et al., 2023) identifies the memory saving of SGD (Robbins and Monro, 1951), fuses the gradient computation and the parameter update in one step. MeZO (Malladi et al., 2023) designs a zeroth-order optimizer to use only two forward passes, which can be used to train a 30B model on a single A100 80GB GPU. These methods waste the superiority of momentum optimizers.

**Parameter-Efficient Fine-tuning** PEFT minimizes resource utilization from the perspective of parameters with addition, selection or decomposition methods (Lialin et al., 2023). The addition-based methods add and update new parameters with the weights of LMs frozen, such as Prefix-Tuning (Li and Liang, 2021), AttentionFusion (Cao et al., 2022), while the added parameters increase the burden on forward propagation. The selection-based methods fine-tune a subset of the parameters of LMs, such as BitFit (Zaken et al., 2022), LT-SFT (Ansell et al., 2022), FAR (Vucetic et al., 2022), but has a performance gap with FPFT. The reparametrization-based methods leverage low-rank decomposition to minimize the number of trainable parameters, such as LoRA (Hu et al., 2022a), PHM (Karimi Mahabadi et al., 2021), KronA (Edalati et al., 2022), S4-model (Chen et al., 2023), while using low-rank representations inevitably leads to information loss and performance degradation. PEFT involves a trade-off between serving efficiency and quality.

**Memory-Efficient Fine-tuning** MEFT minimizes memory usage with heterogeneous memory (e.g., GPU, CPU and NVMe) or parallel methods (e.g., tensor and pipeline parallelism). In a layer-to-layer strategy (Pudipeddi et al., 2020), only the tensors necessary for the computation of a particular layer are transferred to GPU, while the remaining tensors are retained in CPU. ZeRO-Infinity (Rajbhandari et al., 2021) enables the partitioned states and tensors to CPU and NVMe. Tensor parallelism accelerates training by parallelizing tensor computations across different GPUs, but requires multiple global communications during each propagation (Shazeer et al., 2018; Shoeybi et al., 2019). Pipeline parallelism accelerates training by breaking the model into segments or layers and processing them sequentially in a pipeline fashion (Zhang et al.; Kim et al., 2023; Wu et al., 2023). These methods transfer massive memory to het-

erogeneous devices, although temporarily saving memory, still requires a large number of devices.

Different from existing works (Lv et al., 2023; Malladi et al., 2023), HiFT adopts the idea of layer-by-layer training to save memory of FPFT, and can be seamlessly integrated with any optimizer.

### 3 Approach

The overall training strategy of our HiFT is shown in Figure 1. Before elaborating on the details, we first present some necessary notations.

**Notation** Given the training dataset  $\mathcal{D} = \{(x_i, y_i)\}_{i=1}^N$ , the goal of the training is to learn a model  $M$  with  $n$  layers, where  $N$  is the number of the training samples,  $(x_i, y_i)$  is the labeled data pair. We use  $P$  to represent the optimizer, and  $\eta_t$  to represent the learning rate schedule. The number of layers in each group is represented by  $m$  and the number of groups is represented by  $k$ . If  $m$  is divisible by  $n$ , then  $k = n/m$ , otherwise  $k = \lfloor n/m \rfloor + 1$ . Queue  $Q$  is used to store special identifiers that uniquely identify different layers.  $S \in \{\text{"bottom2up"}, \text{"top2down"}, \text{"random"}\}$  represents the adopted update strategy.

Consider a pre-trained LM  $f_{\theta_{pre}}$  parameterized by  $\theta_{pre}$ . Let  $\theta_{fpft}$  and  $\theta_{hi ft}$  denote parameters after full fine-tuning and hierarchical full-parameter fine-tuning after *one training step*, respectively. Let  $\mathcal{L}_\tau(\mathcal{D}; \theta)$  be the objective to minimize during fine-tuning, with  $\mathcal{D}$  being the input,  $\theta$  being updated parameters, and  $\tau$  being the task in fine-tuning. In the process of full fine-tuning, we optimize the model by adjusting its full parameters:

$$\theta_{fpft} = \underset{\theta_{pre}}{\operatorname{argmin}} \mathcal{L}_\tau(\mathcal{D}; \theta_{pre}), \quad (1)$$

where the dimension of  $\theta_{fpft}$ ,  $|\theta_{fpft}|$ , equals the dimension of  $\theta_{pre}$ ,  $|\theta_{pre}|$ .

In the process of HiFT, only a subset of parameters are updated at one training step. More formally, with optimizing group  $i \in \{1, \dots, k\}$ , we have:

$$\theta_{hi ft}^{(i)} = \underset{\beta_i \circ \theta_{hi ft}^{(i-1)}}{\operatorname{argmin}} \mathcal{L}(\mathcal{D}, \beta_i \circ \theta_{hi ft}^{(i-1)} + (1 - \beta_i) \circ \theta_{hi ft}^{(i-1)}) \quad (2)$$

$$\theta_{hi ft}^{(1)} = \underset{\beta_1 \circ \theta_{pre}}{\operatorname{argmin}} \mathcal{L}(\mathcal{D}, \beta_1 \circ \theta_{pre} + (1 - \beta_1) \circ \theta_{pre}), \quad (3)$$

where  $\beta_i$  denotes a fixed binary mask of parameters, with  $\beta_i \in \{0, 1\}^{|\theta_{pre}|}$ , depending on the training strategy chosen in Figure 1. We simply denote  $\theta_{hi ft}^{(k)}$  as  $\theta_{hi ft}$ .

---

**Algorithm 1: HiFT Training Algorithm**

---

**Require:** model  $M$  with  $n$  layers, number of layers per group  $m$ , batch size  $B$ , step budget  $T$ , optimizer  $P$ , parameter queue  $Q$ , update strategy  $S$ , learning rate schedule  $\eta_t$

**Initialize:** Initialize queue  $Q$  by layer identifier  
UpdateStrategy( $Q, S$ )

**for**  $t = 1, \dots, T$  **do**

- a). Freeze all parameters of  $M$ ;
- b). Sample batch  $\mathcal{B} \subset \mathcal{D}$  with random seed  $s$   
*Select key features of layers to be updated*
- c).  $E \leftarrow \text{QueueGetAndRemove}(Q, m)$   
*Removed elements added to tail of queue*
- d).  $\text{QueueAddTail}(Q, E)$
- e).  $\theta_s \leftarrow \text{SelectParameters}(M, E)$
- f). Set `requires_grad = True` of parameters  $\theta_s$
- g).  $\text{UpdateOptimizerParameter}(P, \theta_s)$
- h).  $\text{ForwardPropagation}(M, \mathcal{B})$   
*Preserve optimizer state of  $\theta_s$  within the GPU*
- i).  $\text{MoveOptimizerState2GPU}(P, \theta_s)$
- j).  $\text{Backpropagation}(P, \theta_s, M)$  & Clear gradients  
*Keep optimizer state within the CPU*
- k).  $\text{MoveOptimizerState2CPU}(P, \theta_s)$
- if**  $\text{IsAllLayerUpdate}(t, n, m)$  **then**
  - | Update learning rate  $\eta_t$
- end**
- else**
  - | Keep the learning rate  $\eta_t$  constant
- end**

**end**

---

### 3.1 Hierarchical Training

FPFT has been proven to achieve the state-of-art performance in most downstream tasks (Raschka, 2023; Artur et al., 2023; Kourosh and Rehaan, 2023). Standard FPFT updates all parameters of  $M$  at each training step, which requires a large amount of GPU memory to store forward and backward propagation parameters at the same time. Different from standard FPFT, HiFT only updates a part of the model parameters and freezes the remaining parameters at each training step, and achieves fine-tuning of all parameters through layer-by-layer updates. During the BP process, only the parameters that need to be updated will be stored in the GPU memory, which greatly reduces the GPU memory requirements for FPFT.

As shown in Figure 1, we divide the model into  $k$  groups and update only one group of parameters in each step. All groups are iterated in sequence until convergence. We provide three update strategies: **bottom2up** (B2U), **top2down** (T2D) and **random** (RAN). Different strategies only represent different order of updates, e.g., bottom2up represents the update from the bottom to top. Note that random strategy only shuffles the grouping order before training, and maintains this order in the training

process, which avoids the instability caused by constant changes in the update order. Here, the embedding layer is regarded as the bottom layer, and the head layer used for classification or generation is the top layer.

The detailed training process is shown in Algorithm 1. The first step is to determine the update strategy. During training, we freeze all parameters. The layers to be updated, denoted by  $E$ , are selected from the queue  $Q$  based on the parameter  $m$ . The selected layer  $E$  is removed from head of the queue  $Q$  and added to the tail of  $Q$  to wait for the next update. We select the parameter  $\theta_s$  that needs to be updated from  $M$  based on  $E$ , set the parameter  $\theta_s$  to a computable gradient state and set the update parameter group of optimizer  $P$  to  $\theta_s$ . Before parameter updates, the states parameters (e.g., the gradient first moment estimation and second moment estimation of AdamW) of optimizer  $P$  related to  $\theta_s$  could be moved to GPU devices. After the completion of weight updates, the corresponding gradients are clean up and optimizer states parameters are moved to CPU. To update the learning rate  $\eta_t$ , we employ a delayed update strategy. Specifically, we adjust the learning rate once after updating all layers, which helps alleviate the instability issue arising from excessively updates in some layers, especially when fine-tuning deep models. By employing the successive update strategy, the number of parameters residing in GPU simultaneously reduces, thus lowering the GPU memory requirements of fine-tuned models.

**Note that we provide a theoretical generalization bound for HiFT (Appendix A.1) and memory analysis (Appendix A.2).**

## 4 Experiments

Due to space limitations, please refer to Appendix for datasets (A.3) and experimental setup (A.4).

### 4.1 Baselines

**Language Models** include **RoBERTa** (Liu et al., 2019) with **base** and **large** versions, **GPT-2** (Radford et al., 2019) with **medium** and **large** versions, **LLaMA** (Touvron et al., 2023) with **7B** and **13B** versions, and **OPT-13B** (Zhang et al., 2022).

**Fine-Tuning strategies** include **BitFit** (Zaken et al., 2022), **Adapter** (Houlsby et al., 2019), **Prefix** (Lester et al., 2021), **LoRA** (Hu et al., 2022b), **MeZO** (Malladi et al., 2023), **S4** (Chen et al., 2023), **Adapter<sup>L</sup>** (Lin et al., 2020),

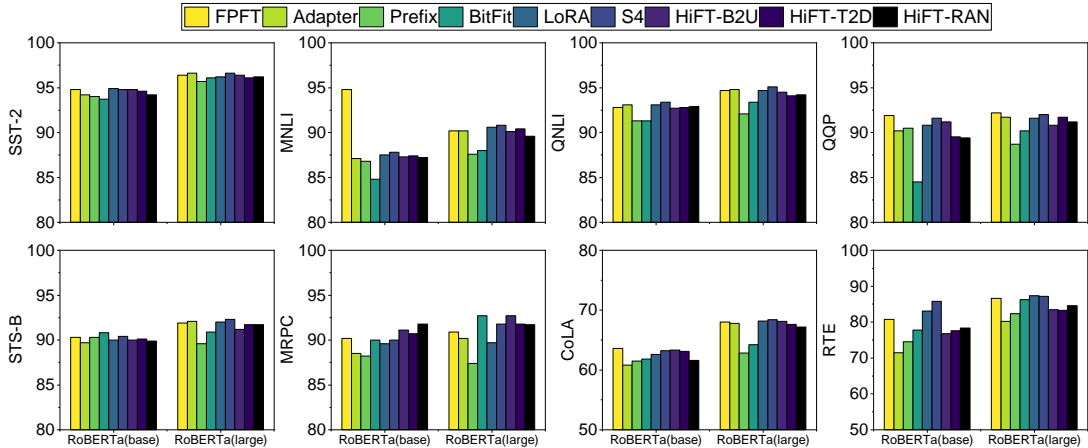


Figure 2: RoBERTa results on different fine-tuning strategies. We report accuracy metrics for the SST-2, QNLI, QQP, MRPC and RTE, mean accuracy for MNLI, spearman coefficient for STS-B and matthews correlation coefficient for CoLA. The  $m$  of HiFT is set to 1. B2U, T2D and RAN are bottom2up, top2down and random strategies.

**PreLayer** (Hu et al., 2022b), and **FPFT**. **Optimizers** include **AdamW** (Loshchilov and Hutter, 2017), **SGDM** (Qian, 1999), **SGD**, **Adafactor** (Shazeer and Stern, 2018), **Adagrad** (Duchi et al., 2010). Some baselines might only appear in certain experiments.

## 4.2 Performance Results

**No prompt results** Figure 2 shows the performance of RoBERTa<sub>base</sub> and RoBERTa<sub>large</sub> using different fine-tuning strategies on eight tasks. The HiFT performances of RoBERTa<sub>base</sub> have competitive advantages with standard FPFT on datasets such as SST-2, MNLI, QNLI and QQP, and HiFT has achieved a weak performance advantage on the MRPC dataset. We observe that HiFT has certain performance advantages on most datasets compared to most PEFT methods such as BitFit, Prefix and Adapter. We get similar conclusions on RoBERTa<sub>large</sub>. The number of layers of model RoBERTa<sub>large</sub> is about twice that of RoBERTa<sub>base</sub>, which reflects to a certain extent that HiFT is not affected by the depth of the model. Table 5 reports the results of GPT-2 including medium and large on the E2E dataset. Compared with standard FPFT, HiFT achieves competitive results on GPT-2 medium and large. Although LoRA has a weak advantage over HiFT in terms of performance, the overall performance of the two is very close.

**Prompt results** MeZO has higher performance under prompt fine-tuning. For a fair comparison, we used prompt templates (see Appendix B.4) of MeZO to perform hierarchical full-parameter fine-tuning. Table 1 reports the prompt-based fine-

tuning results of the RoBERTa<sub>large</sub>. We clearly observe that HiFT has an absolute performance advantage compared to gradient-free methods including MeZO. Compared with standard FPFT and PEFT methods, HiFT still achieves competitive results. Table 2 reports the performance comparison of OPT-13B using different fine-tuning methods on different tasks. We observe that among the 11 tasks, HiFT enjoys performance advantages in 7 tasks. On different task types, HiFT achieves the same or even better performance than standard FPFT, which fully demonstrates the universal effectiveness of HiFT fine-tuning method.

## 4.3 Memory Profiling

To evaluate the effectiveness of HiFT in reducing memory, we conduct extensive experiments on different optimizers (i.e., AdamW, SGDM, SGD, Adafactor and Adagrad) based on multiple LMs including RoBERTa<sub>base</sub>, RoBERTa<sub>large</sub>, GPT-2<sub>large</sub>, GPT-Neo (2.7B), LLaMA-2 (7B) and LLaMA-2 (13B). HiFT reduces memory usage from three aspects: **gradients**, **optimizer states**, and **residual states**. Since HiFT only updates a small number of parameters in each step, this directly reduces the amount of trainable parameters in each training step, and the corresponding gradient parameters and optimizer state parameters also be reduced in the same proportion. When only some layer parameters are updated in each step, the amount of parameters tracking gradients in the calculation graph is reduced, including the amount of parameters in the activations, so HiFT also reduces the amount of parameters in residual states. The reduction in

Task Type	SST-2	SST-5	SNLI	MNLI	RTE	TREC
	— sentiment —		— natural language inference —			— topic —
Zero-shot†	79	35.5	50.2	48.8	51.4	32
<i>Gradient-free methods: k = 16</i>						
LP†	76.0 (2.8)	40.3 (1.9)	66.0 (2.7)	56.5 (2.5)	59.4 (5.3)	51.3 (5.5)
MeZO†	90.5 (1.2)	45.5 (2.0)	68.5 (3.9)	58.7 (2.5)	64.0 (3.3)	76.9 (2.7)
MeZO(LoRA)†	91.4 (0.9)	43.0 (1.6)	69.7 (6.0)	64.0 (2.5)	64.9 (3.6)	73.1 (6.5)
MeZO(prefix)†	90.8 (1.7)	45.8 (2.0)	71.6 (2.5)	63.4 (1.8)	65.4 (3.9)	80.3 (3.6)
MeZO-Adam†	90.4 (1.4)	45.4 (1.5)	74.1 (2.7)	64.3 (0.8)	59.2 (11.1)	78.3 (1.4)
<i>Gradient-based methods: k = 16</i>						
FPFT†	<b>91.9 (1.8)</b>	47.5 (1.9)	77.5 (2.6)	<b>70.0 (2.3)</b>	66.4 (7.2)	85.0 (2.5)
FPFT(LoRA)†	91.4 (1.7)	46.7 (1.1)	74.9 (4.3)	67.7 (1.4)	66.1 (3.5)	82.7 (4.1)
FPFT(prefix)†	<b>91.9 (1.0)</b>	47.7 (1.1)	<b>77.2 (1.3)</b>	66.5 (2.5)	<b>66.6 (2.0)</b>	<b>85.7 (1.3)</b>
HiFT	<b>91.9 (2.3)</b>	<b>47.8 (2.6)</b>	76.7 (3.5)	69.9 (1.9)	66.3 (4.5)	84.3 (4.1)
<i>Gradient-free methods: k = 512</i>						
LP†	91.3 (0.5)	51.7 (0.5)	80.9 (1.0)	71.5 (1.1)	73.1 (1.5)	89.4 (0.5)
MeZO†	93.3 (0.7)	53.2 (1.4)	83.0 (1.0)	78.3 (0.5)	78.6 (2.0)	94.3 (1.3)
MeZO(LoRA)†	93.4 (0.4)	52.4 (0.8)	84.0 (0.8)	77.9 (0.6)	77.6 (1.3)	95.0 (0.7)
MeZO(prefix)†	93.3 (0.1)	53.6 (0.5)	84.8 (1.1)	79.8 (1.2)	77.2 (0.8)	94.4 (0.7)
MeZO-Adam†	93.3 (0.6)	53.9 (0.8)	85.3 (0.8)	79.6 (0.4)	79.2 (1.2)	95.1 (0.3)
<i>Gradient-based methods: k = 512</i>						
FPFT†	93.9 (0.7)	55.9 (0.9)	<b>88.7 (0.8)</b>	<b>84.4 (0.8)</b>	82.7 (1.4)	97.3 (0.2)
FPFT(LoRA)†	<b>94.2 (0.2)</b>	55.3 (0.7)	88.3 (0.5)	83.9 (0.6)	<b>83.2 (1.3)</b>	97.0 (0.3)
FPFT(prefix)†	93.7 (0.3)	54.6 (0.7)	88.3 (0.7)	83.3 (0.5)	82.5 (0.8)	<b>97.4 (0.2)</b>
HiFT	<b>94.2 (0.6)</b>	<b>57.2 (0.8)</b>	88.1 (1.2)	83.8 (0.8)	82.6 (0.9)	96.7 (0.3)

Table 1: Performance of RoBERTa<sub>large</sub> based on prompt fine-tuning. LP: Linear probing; MeZO, MeZO(LoRA) and MeZO(prefix): memory-efficient ZO-SGD with full-parameter tuning, LoRA, and prefix-tuning respectively; FPFT: fine-tuning with AdamW. All reported numbers are averaged accuracy (standard deviation). HiFT uses AdamW and bottom2up strategy. † means the result comes from Malladi et al. (2023)

the number of parameters significantly reduces the GPU memory usage during fine-tuning.

Table 3 reports the memory usage of the parameters, gradients, optimizer states and residual states under FPFT and HiFT for LLaMA-2 (7B). When using the AdamW optimizer and standard mixed precision, HiFT can save about 34.34%-34.46% of memory on RoBERTa<sub>base</sub>, about 35.34%-36.16% of memory on RoBERTa<sub>large</sub>, about 26.92%-27.55% of memory on GPT-2<sub>large</sub>, about 49.65%-54.45% of memory on GPT-Neo and about 57.70%-61.01% of memory on LLaMA compared with FPFT. When using a larger batch size, HiFT is able to save more GPU memory. Please refer to Appendix B for the results of RoBERTa<sub>base</sub> (Table 6), RoBERTa<sub>large</sub> (Table 7), GPT-2<sub>large</sub> (Table 8) and GPT-Neo (2.7B) (Table 9).

Figure 4 shows the percentage of memory used by the parameters of each part when fine-tuning LLaMA (7B) under standard FPFT and HiFT with the AdamW optimizer. Under standard FPFT, the optimizer states occupies the most memory. When fine-tuning 32-bit precision (Figure 4 (a)), the memory occupied by residual states is second only to the

optimizer state. When mixed precision fine-tuning (Figure 4 (c)), the memory used by model parameters exceeds the memory used by residual states is secondary to the optimizer states. The main reason is that in mixed precision training, both 32-bit and half-precision parameters exist at the same time. Therefore, model parameters occupy more memory in mixed precision. HiFT significantly reduces the memory usage of gradients and optimizer states. Therefore, when using HiFT for full-parameter fine-tuning, the main memory-consuming parts are the model parameters and residual states.

We observe an interesting phenomenon when fine-tuning the GPT-Neo (2.7B) (Table 9 in Appendix B) and LLaMA-2 (7B) (Table 3) using mixed precision, the memory usage is higher than FPFT. We find that when using mixed precision fine-tuning, both single-precision and half-precision parameters of the model exist simultaneously. Therefore, the model parameters use more memory in mixed precision than in standard FPFT. Mixed precision mainly focuses on reducing the memory usage of activation states (i.e., residual states). When the model’s own parameter size is

Task	SST2	RTE	CB	BoolQ	WSC	WIC	MultiRC	COPA	ReCoRD	SQuAD	DROP
Task type	classification					multiple choice			generation		
Zero-shot†	58.8	59.6	46.4	59.0	38.5	55.0	46.9	80.0	81.2	46.2	14.6
ICL†	87.0	62.1	57.1	66.9	39.4	50.5	53.1	87.0	<b>82.5</b>	75.9	29.6
LP†	93.4	68.6	67.9	59.3	63.5	60.2	63.5	55.0	27.1	3.7	11.1
MeZO†	91.4	66.1	67.9	67.6	63.5	61.1	60.1	<b>88.0</b>	81.7	84.7	30.9
MeZO (LoRA)†	89.6	67.9	66.1	73.8	<b>64.4</b>	59.7	61.5	84.0	81.2	83.8	31.4
MeZO (prefix)†	90.7	70.8	69.6	73.1	60.6	59.9	63.7	87.0	81.4	84.2	28.9
FPFT†	92.0	70.8	<b>83.9</b>	77.1	63.5	<b>70.1</b>	71.1	79.0	74.1	84.9	31.3
HiFT	<b>94.4</b>	<b>78.7</b>	83.1	<b>78.1</b>	63.6	69.4	<b>71.9</b>	<b>88.0</b>	81.4	<b>86.1</b>	<b>32.7</b>

Table 2: Experiments on OPT-13B (with 1000 examples). ICL: in-context learning; LP: linear probing; FPFT: full fine-tuning; Prefix: prefix-tuning. The parameter  $m$  of HiFT is set to 1. All experiments use prompts in Appendix B.4. † means the result comes from Malladi et al. (2023)

large, the memory increase of the model parameters may be greater than the memory reduction of mixed precision (when the batch size is not large enough). Therefore, it may appear that the memory usage of mixed precision is greater than standard FPFT. Due to the large number of parameters of LLMs (large language models), it is difficult to use larger batch sizes, so it is difficult to bring out the advantages of mixed precision in the context of large models. HiFT is an optional, more efficient solution that maintains single-precision full-parameter fine-tuning while greatly reducing memory usage. We would like to emphasize that the current mixed precision does not support hierarchical operations, so it cannot take advantage of HiFT.

To fully exploit the advantages of HiFT, we have adapted mixed precision to HiFT. That is, each step only moves the single-precision weight corresponding to the parameter that needs to be updated to the GPU (Mixed precision makes a single-precision backup of the weights of the half-precision model.). Table 3 reports the memory profiling for LLaMA2-7B using adapted mixed precision. When using the AdamW optimizer, the adapted mixed precision for HiFT saves approximately 74.87% of GPU memory. When the batch size is 1, fine-tuning the LLaMA-7B model on the E2E data set requires approximately **16.87G** of GPU memory, and fine-tuning the LLaMA-13B model requires approximately 31G of memory. This means that HiFT supports FPFT of a 7B model on a device with 24G GPU memory. Figure 4 (e) reports the changes in the amount of peak fine-tuning parameters under HiFT at different model sizes. We observe that as the number of model parameters increases, the proportion of peak trainable parameters gradually decreases. When fine-tuning the 13B model, the peak amount of fine-tunable parameters is only 2.44% of the original model parameter amount.

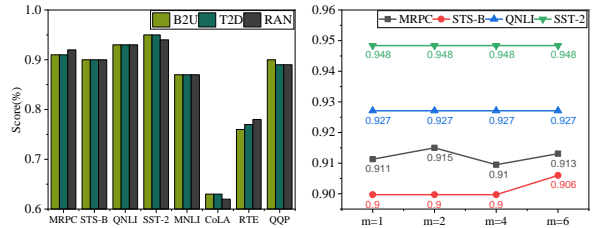


Figure 3: The left shows the performance of HiFT of RoBERTa<sub>base</sub> under **B2U**, **T2D** and **RAN** strategies, respectively. The right shows the performance of HiFT of RoBERTa<sub>base</sub> under different grouping settings, where  $m$  is the number of layers in each group.

#### 4.4 Wallclock Time Efficiency

Table 10 and Table 11 report the running time of fine-tuning RoBERTa and OPT-13B, respectively. We observe that standard full-parameter fine-tuning has a speed advantage over HiFT on RoBERTa<sub>base</sub>, while HiFT has a speed advantage over standard full-parameter fine-tuning on RoBERTa<sub>large</sub>. We believe that the RoBERTa<sub>base</sub> has a small number of parameters and does not reach the computing bottleneck of the GPU. HiFT requires the CPU and GPU to communicate with a small number of parameters, resulting in a slight speed disadvantage. However, for the larger RoBERTa<sub>large</sub> model, HiFT has an absolute speed advantage over standard FPFT. On RoBERTa<sub>large</sub>, the running time of each step of HiFT is in average 1.38 times faster than that of FPFT. Table 11 shows that the average time to fine-tune the OPT-13B on all tasks is approximately 1.32 hours. Under the same batch, the epochs required for hift fine-tuning are generally 2 to 3 times or up to 5 times that of standard FPFT. With larger batches, the fine-tuning time greatly reduces. Compared with the memory advantage brought by HiFT, the weak time disadvantage of our HiFT is acceptable.

Optimizer	#Dtype	#FType	#Trainable				Residual		
			Parameters	#Para(MB)	#Gra(MB)	#Sta(MB)	#PGS(GB)	States(GB)	Total(GB)
AdamW	FP32	FPFT	6738.42M	25705.04	25705.04	51410.08	100.41	41.7	142.11
		HiFT	202.38M	25705.04	772.03	1544.06	27.36	28.04	55.41
	Mixed	FPFT	6738.42M	38557.56	25705.04	51410.08	112.96	32.54	145.50
		HiFT	202.38M	38557.56	772.03	1544.06	39.92	21.62	61.54
	Mixed <sup>Hi</sup>	HiFT	202.38M	13624.53	772.03	1544.06	15.57	21.00	<b>36.57</b>
SGDM	FP32	FPFT	6738.42M	25705.04	25705.04	25705.04	75.31	41.71	117.01
		HiFT	202.38M	25705.04	772.03	772.03	26.61	28.8	55.41
	Mixed	FPFT	6738.42M	38557.56	25705.04	25705.04	87.86	32.54	120.40
		HiFT	202.38M	38557.56	772.03	772.03	39.16	22.37	61.54
	Mixed <sup>Hi</sup>	HiFT	202.38M	13624.53	772.03	772.03	14.81	21.75	<b>36.57</b>
SGD	FP32	FPFT	6738.42M	25705.04	25705.04	0.00	50.21	41.72	91.93
		HiFT	202.38M	25705.04	772.03	0.00	25.86	29.55	55.41
	Mixed	FPFT	6738.42M	38557.56	25705.04	0.00	62.76	32.54	95.30
		HiFT	202.38M	38557.56	772.03	0.00	38.41	23.13	61.54
	Mixed <sup>Hi</sup>	HiFT	202.38M	13624.53	772.03	0.00	14.06	22.51	<b>36.57</b>
Adafactor	FP32	FPFT	6738.42M	25705.04	25705.04	10.82	50.22	41.72	91.94
		HiFT	202.38M	25705.04	772.03	0.33	25.86	29.55	55.41
	Mixed	FPFT	6738.42M	38557.56	25705.04	10.82	62.77	32.54	95.31
		HiFT	202.38M	38557.56	772.03	0.33	38.41	23.13	61.54
	Mixed <sup>Hi</sup>	HiFT	202.38M	13624.53	772.03	0.33	14.06	22.51	<b>36.57</b>
Adagrad	FP32	FPFT	6738.42M	25705.04	25705.04	25705.04	75.31	41.72	117.01
		HiFT	202.38M	25705.04	772.03	772.03	26.61	28.80	55.41
	Mixed	FPFT	6738.42M	38557.56	25705.04	25705.04	87.86	32.54	120.40
		HiFT	202.38M	38557.56	772.03	772.03	39.16	22.37	61.54
	Mixed <sup>Hi</sup>	HiFT	202.38M	13624.53	772.03	772.03	14.81	21.75	<b>36.57</b>

Table 3: The GPU memory usage of fine-tuning LLaMA (7B) on the E2E dataset. The sequence length and batch size are set to 512 and 6, respectively. **#Dtype** represents the data type used for training, where **FP32** represents fully parameter fine-tuning the model with 32-bit precision, **mixed** represents fine-tuning with standard mixed precision and **mixed<sup>Hi</sup>** represents the mixed precision adapted to HiFT. **#Trainable parameters** represents the maximum number of trainable parameters that appear in a single step during the fine-tuning process. **#Para** represents the memory occupied by the model parameters, **#Gra** represents the memory occupied by the gradient, and **#Sta** represents the memory occupied by the optimizer state. **#PGS** represents the sum of memory occupied by model parameters (i.e.,**#Para**), gradients (i.e.,**#Gra**) and optimizer state (i.e.,**#Sta**). **Residual states** mainly includes activation, temporary buffers and unusable fragmented memory. **Total** represents the total memory used during fine-tuning. The parameter  $m$  of HiFT is set to 1.

#### 4.5 Impact of Strategy

The left plot of Figure 3 reports the performance of RoBERTa<sub>base</sub> using B2U, T2D and RAN strategies. We observe that the order of updates has almost no effect on the performance of the model. It is an interesting phenomenon that the model still achieves competitive results even when updated in a random order. Changing the update order does not affect the position of the corresponding layer in the model, which is the reason why the performance is not affected. We believe that this phenomenon provides support for hierarchical parallel fine-tuning of large-scale models in the future.

#### 4.6 Impact of Grouping

The right plot of Figure 3 reports the impact of different grouping settings on model performance. Although different grouping settings can cause fluctuations in model performance, the overall impact is negligible. We use the learning rate delayed update strategy, which updates the learning rate

only after all layers are updated once. This strategy ensures that the learning rate used to update the parameters of each layer is the same in each training step, which helps to prevent the model performance from decreasing due to the update of some parameters being too fast in the hierarchical update process.

#### Conclusion

In this paper, we propose an end-to-end hierarchical full-parameter fine-tuning strategy, HiFT, which groups the model parameters and updates a single group of parameters per training step. The number of trainable parameters per training step greatly reduce, which lowers the GPU memory usage of the corresponding gradients, optimizer state parameters, and activations. HiFT lowers the barrier of full-parameter fine-tuning of language models and supports full-parameter fine-tuning of a 7B model on a 24G memory device.



## Limitations

Although HiFT achieves the performance of standard full-parameter fine-tuning at a lower GPU memory cost, there are still some shortcomings. HiFT divides the model by layers, and the maximum division limit is the number of layers of the model. Due to the limitation of the number of layers, HiFT cannot break through the number of model layers for finer-grained division. When the model width is large, it limits HiFT’s capabilities. On the other hand, after dividing the model, the number of parameters in each group is different, and the GPU memory usage fluctuates during the fine-tuning process. The peak memory occupied by the fine-tuned model is the decisive factor that determines whether the model is able to be fine-tuned on a certain device. This fluctuation in memory usage during fine-tuning prevents us from fully utilizing resources.

## References

- Alan Ansell, Edoardo Ponti, Anna Korhonen, and Ivan Vulić. 2022. Composable sparse fine-tuning for cross-lingual transfer. In *Proceedings of the 60th Annual Meeting of the Association for Computational Linguistics (Volume 1: Long Papers)*, pages 1778–1796.
- Niederfahnenhorst Artur, Hakhamaneshi Kourosh, and Ahmad Rehaan. 2023. *Fine-Tuning LLMs: LoRA or Full-Parameter? An in-depth Analysis with Llama-2*.
- Yoshua Bengio, Pascal Lamblin, Dan Popovici, and Hugo Larochelle. 2006. Greedy layer-wise training of deep networks. *Advances in neural information processing systems*, 19.
- Jin Cao, Chandana Satya Prakash, and Wael Hamza. 2022. Attention fusion: a light yet efficient late fusion mechanism for task adaptation in nlu. In *Findings of the Association for Computational Linguistics: NAACL 2022*, pages 857–866.
- Daniel Cer, Mona Diab, Eneko Agirre, Iñigo Lopez-Gazpio, and Lucia Specia. 2017. Semeval-2017 task 1: Semantic textual similarity multilingual and crosslingual focused evaluation. In *Proceedings of the 11th International Workshop on Semantic Evaluation (SemEval-2017)*, pages 1–14.
- Jiaao Chen, Aston Zhang, Xingjian Shi, Mu Li, Alex Smola, and Diyi Yang. 2023. Parameter-efficient fine-tuning design spaces. *arXiv preprint arXiv:2301.01821*.
- Tianqi Chen, Bing Xu, Chiyuan Zhang, and Carlos Guestrin. 2016. [Training deep nets with sublinear memory cost](#). *ArXiv*, abs/1604.06174.
- Christopher Clark, Kenton Lee, Ming-Wei Chang, Tom Kwiatkowski, Michael Collins, and Kristina Toutanova. 2019. Boolq: Exploring the surprising difficulty of natural yes/no questions. In *Proceedings of the 2019 Conference of the North American Chapter of the Association for Computational Linguistics: Human Language Technologies, Volume 1 (Long and Short Papers)*, pages 2924–2936.
- Marie-Catherine De Marneffe, Mandy Simons, and Judith Tonhauser. 2019. The commitmentbank: Investigating projection in naturally occurring discourse. In *proceedings of Sinn und Bedeutung*, volume 23, pages 107–124.
- Dheeru Dua, Yizhong Wang, Pradeep Dasigi, Gabriel Stanovsky, Sameer Singh, and Matt Gardner. 2019. Drop: A reading comprehension benchmark requiring discrete reasoning over paragraphs. In *Proceedings of the 2019 Conference of the North American Chapter of the Association for Computational Linguistics: Human Language Technologies, Volume 1 (Long and Short Papers)*, pages 2368–2378.
- John C. Duchi, Elad Hazan, and Yoram Singer. 2010. Adaptive subgradient methods for online learning and stochastic optimization. In *COLT 2010 - The 23rd Conference on Learning Theory, Haifa, Israel, June 27-29, 2010*, pages 257–269. Omnipress.
- Ali Edalati, Marzieh Tahaei, Ivan Kobyzev, Vahid Par-tovi Nia, James J Clark, and Mehdi Rezagholizadeh. 2022. Krona: Parameter efficient tuning with kronecker adapter. *arXiv preprint arXiv:2212.10650*.
- Tianyu Gao, Adam Fisch, and Danqi Chen. 2021. [Making pre-trained language models better few-shot learners](#). In *Proceedings of the 59th Annual Meeting of the Association for Computational Linguistics and the 11th International Joint Conference on Natural Language Processing (Volume 1: Long Papers)*, pages 3816–3830, Online. Association for Computational Linguistics.
- Neil Houlsby, Andrei Giurgiu, Stanislaw Jastrzebski, Bruna Morrone, Quentin De Laroussilhe, Andrea Gesmundo, Mona Attariyan, and Sylvain Gelly. 2019. Parameter-efficient transfer learning for nlp. In *International Conference on Machine Learning*, pages 2790–2799. PMLR.
- Edward J. Hu, Yelong Shen, Phillip Wallis, Zeyuan Allen-Zhu, Yuanzhi Li, Shean Wang, Lu Wang, and Weizhu Chen. 2022a. [Lora: Low-rank adaptation of large language models](#). In *The Tenth International Conference on Learning Representations, ICLR 2022, Virtual Event, April 25-29, 2022*. OpenReview.net.
- Edward J. Hu, Yelong Shen, Phillip Wallis, Zeyuan Allen-Zhu, Yuanzhi Li, Shean Wang, Lu Wang, and Weizhu Chen. 2022b. Lora: Low-rank adaptation of large language models. In *The Tenth International Conference on Learning Representations, ICLR 2022, Virtual Event, April 25-29, 2022*. OpenReview.net.

- Rabeeh Karimi Mahabadi, James Henderson, and Sebastian Ruder. 2021. Compacter: Efficient low-rank hypercomplex adapter layers. *Advances in Neural Information Processing Systems*, 34:1022–1035.
- Daniel Khashabi, Snigdha Chaturvedi, Michael Roth, Shyam Upadhyay, and Dan Roth. 2018. Looking beyond the surface: A challenge set for reading comprehension over multiple sentences. In *Proceedings of the 2018 Conference of the North American Chapter of the Association for Computational Linguistics: Human Language Technologies, Volume 1 (Long Papers)*, pages 252–262.
- Taebum Kim, Hyoungjoo Kim, Gyeong-In Yu, and Byung-Gon Chun. 2023. Bpipe: Memory-balanced pipeline parallelism for training large language models. In *International Conference on Machine Learning, ICML 2023, 23-29 July 2023, Honolulu, Hawaii, USA*, volume 202 of *Proceedings of Machine Learning Research*, pages 16639–16653. PMLR.
- Hakhamaneshi Kourosh and Ahmad Rehaan. 2023. [Fine-Tuning Llama-2: A Comprehensive Case Study for Tailoring Models to Unique Applications](#).
- Brian Lester, Rami Al-Rfou, and Noah Constant. 2021. The power of scale for parameter-efficient prompt tuning. In *Proceedings of the 2021 Conference on Empirical Methods in Natural Language Processing*, pages 3045–3059.
- Hector Levesque, Ernest Davis, and Leora Morgenstern. 2012. The winograd schema challenge. In *Thirteenth international conference on the principles of knowledge representation and reasoning*.
- Mike Lewis, Yinhan Liu, Naman Goyal, Marjan Ghazvininejad, Abdelrahman Mohamed, Omer Levy, Veselin Stoyanov, and Luke Zettlemoyer. 2020. BART: denoising sequence-to-sequence pre-training for natural language generation, translation, and comprehension. In *Proceedings of the 58th Annual Meeting of the Association for Computational Linguistics, ACL 2020, Online, July 5-10, 2020*, pages 7871–7880. Association for Computational Linguistics.
- Xiang Lisa Li and Percy Liang. 2021. Prefix-tuning: Optimizing continuous prompts for generation. In *Proceedings of the 59th Annual Meeting of the Association for Computational Linguistics and the 11th International Joint Conference on Natural Language Processing (Volume 1: Long Papers)*, pages 4582–4597.
- Vladislav Lialin, Vijeta Deshpande, and Anna Rumshisky. 2023. Scaling down to scale up: A guide to parameter-efficient fine-tuning. *arXiv preprint arXiv:2303.15647*.
- Peiqin Lin, Shaoxiong Ji, Jörg Tiedemann, André FT Martins, and Hinrich Schütze. 2024. Mala-500: Massive language adaptation of large language models. *arXiv preprint arXiv:2401.13303*.
- Zhaojiang Lin, Andrea Madotto, and Pascale Fung. 2020. Exploring versatile generative language model via parameter-efficient transfer learning. In *Findings of the Association for Computational Linguistics: EMNLP 2020*, pages 441–459.
- Yinhan Liu, Jiatao Gu, Naman Goyal, Xian Li, Sergey Edunov, Marjan Ghazvininejad, Mike Lewis, and Luke Zettlemoyer. 2020. Multilingual denoising pre-training for neural machine translation. *Trans. Assoc. Comput. Linguistics*, 8:726–742.
- Yinhan Liu, Myle Ott, Naman Goyal, Jingfei Du, Mandar Joshi, Danqi Chen, Omer Levy, Mike Lewis, Luke Zettlemoyer, and Veselin Stoyanov. 2019. Roberta: A robustly optimized BERT pretraining approach. *CoRR*, abs/1907.11692.
- Ilya Loshchilov and Frank Hutter. 2017. [Decoupled weight decay regularization](#). In *International Conference on Learning Representations*.
- Kai Lv, Yuqing Yang, Tengxiao Liu, Qinghui Gao, Qipeng Guo, and Xipeng Qiu. 2023. Full parameter fine-tuning for large language models with limited resources. *CoRR*, abs/2306.09782.
- Bolei Ma, Ercong Nie, Shuzhou Yuan, Helmut Schmid, Michael Färber, Frauke Kreuter, and Hinrich Schütze. 2024. Topro: Token-level prompt decomposition for cross-lingual sequence labeling tasks. *arXiv preprint arXiv:2401.16589*.
- Sadhika Malladi, Tianyu Gao, Eshaan Nichani, Alex Damian, Jason D. Lee, Danqi Chen, and Sanjeev Arora. 2023. Fine-tuning language models with just forward passes. *CoRR*, abs/2305.17333.
- Vaishnavh Nagarajan and J. Zico Kolter. 2019. [Uniform convergence may be unable to explain generalization in deep learning](#). *CoRR*, abs/1902.04742.
- Deepak Narayanan, Mohammad Shoeybi, Jared Casper, Patrick LeGresley, Mostofa Patwary, Vijay Korthikanti, Dmitri Vainbrand, Prethvi Kashinkunti, Julie Bernauer, Bryan Catanzaro, Amar Phanishayee, and Matei Zaharia. 2021. Efficient large-scale language model training on GPU clusters using megatron-lm. In *International Conference for High Performance Computing, Networking, Storage and Analysis, SC 2021, St. Louis, Missouri, USA, November 14-19, 2021*, page 58. ACM.
- Jekaterina Novikova, Ondřej Dušek, and Verena Rieser. 2017. The e2e dataset: New challenges for end-to-end generation. In *Proceedings of the 18th Annual SIGdial Meeting on Discourse and Dialogue*, pages 201–206.
- Abhishek Panigrahi, Nikunj Saunshi, Haoyu Zhao, and Sanjeev Arora. 2023. [Task-specific skill localization in fine-tuned language models](#). In *International Conference on Machine Learning, ICML 2023, 23-29 July 2023, Honolulu, Hawaii, USA*, volume 202 of *Proceedings of Machine Learning Research*, pages 27011–27033. PMLR.

- Mohammad Taher Pilehvar and Jose Camacho-Collados. 2019. Wic: the word-in-context dataset for evaluating context-sensitive meaning representations. In *Proceedings of the 2019 Conference of the North American Chapter of the Association for Computational Linguistics: Human Language Technologies, Volume 1 (Long and Short Papers)*, pages 1267–1273.
- Bharadwaj Pudipeddi, Maral Mesmakhosroshahi, Jintwen Xi, and Sujeeth Bharadwaj. 2020. Training large neural networks with constant memory using a new execution algorithm. *CoRR*, abs/2002.05645.
- Ning Qian. 1999. On the momentum term in gradient descent learning algorithms. *Neural Networks*, 12(1):145–151.
- Alec Radford, Jeff Wu, Rewon Child, David Luan, Dario Amodei, and Ilya Sutskever. 2019. Language models are unsupervised multitask learners.
- Samyam Rajbhandari, Jeff Rasley, Olatunji Ruwase, and Yuxiong He. 2020a. Zero: memory optimizations toward training trillion parameter models. In *Proceedings of the International Conference for High Performance Computing, Networking, Storage and Analysis, SC 2020, Virtual Event / Atlanta, Georgia, USA, November 9-19, 2020*, page 20. IEEE/ACM.
- Samyam Rajbhandari, Jeff Rasley, Olatunji Ruwase, and Yuxiong He. 2020b. Zero: Memory optimizations toward training trillion parameter models. In *SC20: International Conference for High Performance Computing, Networking, Storage and Analysis*, pages 1–16. IEEE.
- Samyam Rajbhandari, Olatunji Ruwase, Jeff Rasley, Shaden Smith, and Yuxiong He. 2021. Zero-infinity: breaking the GPU memory wall for extreme scale deep learning. In *International Conference for High Performance Computing, Networking, Storage and Analysis, SC 2021, St. Louis, Missouri, USA, November 14-19, 2021*, page 59. ACM.
- Pranav Rajpurkar, Robin Jia, and Percy Liang. 2018. Know what you don’t know: Unanswerable questions for squad. In *Proceedings of the 56th Annual Meeting of the Association for Computational Linguistics (Volume 2: Short Papers)*, pages 784–789.
- Pranav Rajpurkar, Jian Zhang, Konstantin Lopyrev, and Percy Liang. 2016. Squad: 100,000+ questions for machine comprehension of text. In *Proceedings of the 2016 Conference on Empirical Methods in Natural Language Processing*, pages 2383–2392.
- Sebastian Raschka. 2023. *Finetuning LLMs with LoRA and QLoRA: Insights from Hundreds of Experiments*.
- Herbert Robbins and Sutton Monro. 1951. A stochastic approximation method. *The Annals of Mathematical Statistics*, 22(3):400–407.
- Melissa Roemmele, Cosmin Adrian Bejan, and Andrew S Gordon. 2011. Choice of plausible alternatives: An evaluation of commonsense causal reasoning. In *2011 AAAI Spring Symposium Series*.
- Noam Shazeer, Youlong Cheng, Niki Parmar, Dustin Tran, Ashish Vaswani, Penporn Koanantakool, Peter Hawkins, Hyoungho Lee, Mingsheng Hong, Cliff Young, Ryan Sepassi, and Blake A. Hechtman. 2018. Mesh-tensorflow: Deep learning for supercomputers. In *Advances in Neural Information Processing Systems 31: Annual Conference on Neural Information Processing Systems 2018, NeurIPS 2018, December 3-8, 2018, Montréal, Canada*, pages 10435–10444.
- Noam Shazeer and Mitchell Stern. 2018. Adafactor: Adaptive learning rates with sublinear memory cost. In *Proceedings of the 35th International Conference on Machine Learning, ICML 2018, Stockholm, Sweden, July 10-15, 2018*, volume 80 of *Proceedings of Machine Learning Research*, pages 4603–4611. PMLR.
- Sheng Shen, Pete Walsh, Kurt Keutzer, Jesse Dodge, Matthew E. Peters, and Iz Beltagy. 2022. Staged training for transformer language models. In *International Conference on Machine Learning, ICML 2022, 17-23 July 2022, Baltimore, Maryland, USA*, volume 162 of *Proceedings of Machine Learning Research*, pages 19893–19908. PMLR.
- Mohammad Shoeybi, Mostofa Patwary, Raul Puri, Patrick LeGresley, Jared Casper, and Bryan Catanzaro. 2019. Megatron-lm: Training multi-billion parameter language models using model parallelism. *CoRR*, abs/1909.08053.
- Richard Socher, Alex Perelygin, Jean Wu, Jason Chuang, Christopher D Manning, Andrew Y Ng, and Christopher Potts. 2013. Recursive deep models for semantic compositionality over a sentiment treebank. In *Proceedings of the 2013 conference on empirical methods in natural language processing*, pages 1631–1642.
- Xianghui Sun, Yunjie Ji, Baochang Ma, and Xianggang Li. 2023. A comparative study between full-parameter and lora-based fine-tuning on chinese instruction data for instruction following large language model. *CoRR*, abs/2304.08109.
- Hugo Touvron, Louis Martin, Kevin Stone, Peter Albert, Amjad Almahairi, Yasmine Babaei, Nikolay Bashlykov, Soumya Batra, Prajjwal Bhargava, Shrutik Bhosale, Dan Bikel, Lukas Blecher, Cristian Canton-Ferrer, Moya Chen, Guillem Cucurull, David Esiobu, Jude Fernandes, Jeremy Fu, Wenyin Fu, Brian Fuller, Cynthia Gao, Vedanuj Goswami, Naman Goyal, Anthony Hartshorn, Saghar Hosseini, Rui Hou, Hakan Inan, Marcin Kardas, Viktor Kerkez, Madian Khabsa, Isabel Kloumann, Artem Korenev, Punit Singh Koura, Marie-Anne Lachaux, Thibaut Lavril, Jenya Lee, Diana Liskovich, Yinghai Lu, Yuning Mao, Xavier Martinet, Todor Mihaylov, Pushkar Mishra, Igor Molybog, Yixin Nie, Andrew Poulton, Jeremy Reizenstein, Rashi Rungta, Kalyan Saladi, Alan Schelten, Ruan Silva, Eric Michael Smith, Ranjan Subramanian, Xiaoqing Ellen Tan, Binh Tang, Ross Taylor, Adina Williams, Jian Xiang Kuan, Puxin Xu, Zheng Yan, Iliyan Zarov, Yuchen Zhang, Angela Fan,

- Melanie Kambadur, Sharan Narang, Aurélien Rodriguez, Robert Stojnic, Sergey Edunov, and Thomas Scialom. 2023. Llama 2: Open foundation and fine-tuned chat models. *CoRR*, abs/2307.09288.
- Ashish Vaswani, Noam Shazeer, Niki Parmar, Jakob Uszkoreit, Llion Jones, Aidan N Gomez, Łukasz Kaiser, and Illia Polosukhin. 2017. Attention is all you need. In *Advances in Neural Information Processing Systems*, volume 30. Curran Associates, Inc.
- Danilo Vucetic, Mohammadreza Tayaraniyan, Maryam Ziaeeafard, James J Clark, Brett H Meyer, and Warren J Gross. 2022. Efficient fine-tuning of bert models on the edge. In *2022 IEEE International Symposium on Circuits and Systems (ISCAS)*, pages 1838–1842. IEEE.
- Alex Wang, Amanpreet Singh, Julian Michael, Felix Hill, Omer Levy, and Samuel R. Bowman. 2018. [Glue: A multi-task benchmark and analysis platform for natural language understanding](#). In *BlackboxNLP:EMNLP*.
- Alex Warstadt, Amanpreet Singh, and Samuel R Bowman. 2019. Neural network acceptability judgments. *Transactions of the Association for Computational Linguistics*, 7:625–641.
- Adina Williams, Nikita Nangia, and Samuel R Bowman. 2018. A broad-coverage challenge corpus for sentence understanding through inference. In *Proceedings of NAACL-HLT*, pages 1112–1122.
- Shaohua Wu, Xudong Zhao, Shenling Wang, Jiangang Luo, Lingjun Li, Xi Chen, Bing Zhao, Wei Wang, Tong Yu, Rongguo Zhang, Jiahua Zhang, and Chao Wang. 2023. YUAN 2.0: A large language model with localized filtering-based attention. *CoRR*, abs/2311.15786.
- Elad Ben Zaken, Yoav Goldberg, and Shauli Ravfogel. 2022. Bitfit: Simple parameter-efficient fine-tuning for transformer-based masked language-models. In *Proceedings of the 60th Annual Meeting of the Association for Computational Linguistics (Volume 2: Short Papers)*, pages 1–9.
- Sheng Zhang, Xiaodong Liu, Jingjing Liu, Jianfeng Gao, Kevin Duh, and Benjamin Van Durme. 2018. Record: Bridging the gap between human and machine commonsense reading comprehension. *arXiv preprint arXiv:1810.12885*.
- Susan Zhang, Stephen Roller, Naman Goyal, Mikel Artetxe, Moya Chen, Shuohui Chen, Christopher Dewan, Mona T. Diab, Xian Li, Xi Victoria Lin, Todor Mihaylov, Myle Ott, Sam Shleifer, Kurt Shuster, Daniel Simig, Punit Singh Koura, Anjali Sridhar, Tianlu Wang, and Luke Zettlemoyer. 2022. OPT: open pre-trained transformer language models. *CoRR*, abs/2205.01068.
- Zheng Zhang, Donglin Yang, Yaqi Xia, Liang Ding, Dacheng Tao, Xiaobo Zhou, and Dazhao Cheng. Mpipemoe: Memory efficient moe for pre-trained models with adaptive pipeline parallelism. In *IEEE International Parallel and Distributed Processing Symposium, IPDPS 2023, St. Petersburg, FL, USA, May 15-19, 2023*, pages 167–177. IEEE.

## A Appendix

### A.1 Generalization Bound for HiFT

In this section, we establish the generalization bound for HiFT, first building upon a quantization assumption as in Panigrahi et al. (2023). It is important to note that quantization is a common practical consideration; for instance, in our work, we implement a 32-bit quantization precision.

**Assumption 1.** (Quantization bound) *Given model parameters  $\theta$ , we denote  $\bar{q}(\theta)$  to be the parameter that quantizes every parameter into the  $q$  given values. Then there exist  $\varepsilon > 0$  s.t. for any sample  $x_i$  with label  $y_i$  at any training step, we have*

$$|\mathcal{L}((x_i, y_i); \bar{q}(\theta)) - \mathcal{L}((x_i, y_i); \theta)| \leq \varepsilon. \quad (4)$$

**Assumption 2.** (Uniform convergence generalization bound for subset parameter fine-tuning) *Following Panigrahi et al. (2023), we deviate from the classical uniform convergence generalization bound (Nagarajan and Kolter, 2019) to get a tighter uniform convergence generalization bound for HiFT:*

$$\begin{aligned} \mathcal{L}_{test}(\theta_{hi\!ft}^{(i)}) - \mathcal{L}_{train}(\theta_{hi\!ft}^{(i)}) \\ \leq \sup_{\tilde{\theta}_{hi\!ft}^{(i)} \in \Theta} |\mathcal{L}_{test}(\tilde{\theta}_{hi\!ft}^{(i)}) - \mathcal{L}_{train}(\tilde{\theta}_{hi\!ft}^{(i)})|, \end{aligned} \quad (5)$$

where  $\Theta$  denotes the subset of parameter space,  $\theta_{hi\!ft}^{(i)}$  being the parameter after  $i$ -th optimizing step at one training step.

**Theorem 3.** (HiFT generalization bound) *Under Assumption 1 and 2, we have the following generalization bound for HiFT:*

$$\begin{aligned} \mathcal{L}_{test}(\theta_{hi\!ft}^{(k)}) - \mathcal{L}_{test}(\theta^*) \\ \leq 4k\varepsilon + 2 \sum_{i=1}^k \sup_{\tilde{\theta}^{(i)}} |\mathcal{L}_{test}(\bar{q}(\tilde{\theta}^{(i)})) - \mathcal{L}_{train}(\bar{q}(\tilde{\theta}^{(i)}))| \\ + \mathcal{L}_{test}(\theta^{(k)*}) - \mathcal{L}_{test}(\theta^*), \end{aligned} \quad (6)$$

where  $\theta^*$  denotes the parameter with the best test performance,  $\tilde{\theta}^{(i)}$  is in the space of  $\beta_i \circ \theta_{pre}$  and  $\theta^{(i)*}$  denotes the parameter with the best test performance when only changing the subset parameter  $\beta_i \circ \theta_{pre}$ . With probability at least  $1 - \delta$ , the second term  $2 \sum_{i=1}^k \sup_{\tilde{\theta}^{(i)}} |\mathcal{L}_{test}(\bar{q}(\tilde{\theta}^{(i)})) - \mathcal{L}_{train}(\bar{q}(\tilde{\theta}^{(i)}))|$  can be further bounded:

$$\begin{aligned} 2 \sum_{i=1}^k \sup_{\tilde{\theta}^{(i)}} |\mathcal{L}_{test}(\bar{q}(\tilde{\theta}^{(i)})) - \mathcal{L}_{train}(\bar{q}(\tilde{\theta}^{(i)}))| \\ \leq 2 \sum_{i=1}^k \sqrt{\frac{s_i \log q + \log(1/\delta)}{N}}, \end{aligned} \quad (7)$$

where  $s_i$  denotes the number of parameters in each optimizing group  $i$ .

*Proof.* We first derive HiFT generalization bound between the objective with parameters after a first step of optimization at one training step  $\mathcal{L}_{test}(\theta_{hi\!ft}^{(1)})$  and the objective with parameters that has the best test performance  $\mathcal{L}_{test}(\theta^*)$ :

$$\begin{aligned} \mathcal{L}_{test}(\theta_{hi\!ft}^{(1)}) - \mathcal{L}_{test}(\theta^*) \\ \leq 4\varepsilon \\ + 2 \sup_{\tilde{\theta}^{(1)}} |\mathcal{L}_{test}(\bar{q}(\tilde{\theta}^{(1)})) - \mathcal{L}_{train}(\bar{q}(\tilde{\theta}^{(1)}))| \\ + \mathcal{L}_{test}(\theta^{(1)*}) - \mathcal{L}_{test}(\theta^*), \end{aligned} \quad (8)$$

with probability at least  $1 - \delta$ , the second term can be bounded:

$$\begin{aligned} 2 \sup_{\tilde{\theta}^{(1)}} |\mathcal{L}_{test}(\bar{q}(\tilde{\theta}^{(1)})) - \mathcal{L}_{train}(\bar{q}(\tilde{\theta}^{(1)}))| \\ \leq 2 \sqrt{\frac{s_1 \log q + \log(1/\delta)}{N}} \end{aligned} \quad (9)$$

The above inequality can be shown by considering Theorem D.2 in Panigrahi et al. (2023) and taking  $\Theta_N = 1$ .

Similarly, we can have:

$$\begin{aligned} \mathcal{L}_{test}(\theta_{hi\!ft}^{(i)}) - \mathcal{L}_{test}(\theta_{hi\!ft}^{(i-1)}) \\ \leq 4\varepsilon \\ + 2 \sup_{\tilde{\theta}^{(i)}} |\mathcal{L}_{test}(\bar{q}(\tilde{\theta}^{(i)})) - \mathcal{L}_{train}(\bar{q}(\tilde{\theta}^{(i)}))| \\ + \mathcal{L}_{test}(\theta^{(i)*}) - \mathcal{L}_{test}(\theta_{hi\!ft}^{(i-1)}) \end{aligned} \quad (10)$$

Summing over the above terms with  $i = \{1, \dots, k\}$  completes the proof of this theorem.

### A.2 Memory Analysis

According to previous work (Lv et al., 2023; Malladi et al., 2023), the main components that consume GPU memory during the fine-tuning process include the weight parameter, optimizer states, gradients, and calculation of residual states (i.e. activations, temporary buffers and fragmented memory) (Rajbhandari et al., 2020b). In this section, we give theoretical analysis on the GPU memory advantages of HiFT strategy from the perspectives of **weight parameter**, **optimizer states** and **gradients**<sup>1</sup>. Assuming the model is fine-tuned using the AdamW optimizer with 32-bit precision, we employ  $W_1$ ,  $W_2$ ,  $W_3$  to represent weight parameter, optimizer states and gradients respectively.

<sup>1</sup>Since the GPU memory occupied by forward activations is related to the model implementation, batch size and sentence length, we analyze the GPU memory requirements of internal variables through experiments.

AdamW optimizer stores the gradient first moment estimation and second moment estimation, which means that the optimizer state parameter  $W_2$  is two times larger than weight parameter  $W_1$  (i.e.,  $W_2 = 2 * W_1$ ). The gradient parameters typically correspond to the parameters updated in the model (i.e.,  $W_3 = W_1$ ). Therefore, the number of gradient parameters  $W_3$  is the same as the number of parameters  $W_1$  that need to be updated in the model. Therefore, for standard FPFT, the GPU memory required for these parameters is as follows:

$$\begin{aligned} \mathcal{W}_{fpft} &= W_1 + W_2 + W_3 \\ &= W_1 + 2W_1 + W_1 \\ &= 4W_1 \end{aligned} \quad (11)$$

Taking the fine-tuning of LLaMA-7B at 32 precision using the AdamW optimizer as an example, the  $W_1$  parameter is about 26.08G. Theoretically, the GPU memory required for fine-tuning these three parts of the 7B model is approximately 104.32 GB. If considering GPU memory occupied by forward activations and the impact of batch size and sentence length (Lv et al., 2023), the actual scenario FPFT requires more GPU memory than 104.32 GB. Under the HiFT training strategy, since only one group of parameters is updated for each training step, only the gradients of the updated parameters and the corresponding optimizer states are stored in the GPU according to Algorithm 1. The weight parameter need to reside in the GPU memory for forward propagation. Therefore, the average GPU memory required for each training step is as follows:

$$\begin{aligned} \mathcal{W}_{hift} &= W_1 + \frac{W_2}{k} + \frac{W_3}{k} \\ &= \frac{k+3}{k} * W_1 \end{aligned} \quad (12)$$

Compared with FPFT, the memory saved by HiFT in model parameters, gradients and optimizer states is:

$$\begin{aligned} \Delta \mathcal{W} &= \mathcal{W}_{pft} - \mathcal{W}_{hift} \\ &= \frac{3k-3}{k} * W_1 \end{aligned} \quad (13)$$

In addition to these computable fixed parameters, HiFT can reduce the number of activation-related parameters that simultaneously reside in memory, which is discussed in the experimental section. Considering the embedding layer, task-related head layer and 32 hidden layers, LLaMA-7B has  $n = 34$

layers. When  $m = 1$ , it can be deduced that  $k = 34$ , and the required GPU memory can be inferred to be  $\mathcal{W}_{hift} \approx 31.13G$ , the GPU memory saving is about 73.19G compared with FPFT.

### A.3 Datasets

We conduct experiments on the following datasets: **GLUE** (Wang et al., 2018) (SST-2 (Socher et al., 2013), CoLA (Warstadt et al., 2019), MNLI (Williams et al., 2018), MRPC (Warstadt et al., 2019), QNLI (Rajpurkar et al., 2018), QQP<sup>2</sup>, RTE and STS-B (Cer et al., 2017)); **SuperGLUE** (CB (De Marneffe et al., 2019), BoolQ (Clark et al., 2019), COPA (Roemmele et al., 2011), MultiRC (Khashabi et al., 2018), RTE, WiC (Pilehvar and Camacho-Collados, 2019), WSC (Levesque et al., 2012), ReCoRD (Zhang et al., 2018)), **SQuAD** (Rajpurkar et al., 2016), **E2E** (Novikova et al., 2017) and **DROP** (Dua et al., 2019). We conduct memory profiling using CoLA and E2E datasets as examples.

### A.4 Implementation Details

The performance results of the experiment are based on training with the AdamW optimizer. For RoBERTa<sub>base</sub> and RoBERTa<sub>large</sub> models, we follow Chen et al. (2023) for the hyperparameter setting of no-prompt fine-tuning such as batch size and learning rate. For GPT-2<sub>medium</sub> and GPT-2<sub>large</sub>, we follow Hu et al. (2022b) for the hyperparameter setting for no-prompt fine-tuning such as batch size and learning rate. For RoBERTa<sub>large</sub> model, we follow Malladi et al. (2023) for the hyperparameter setting of prompt fine-tuning such as prompt template, batch size and learning rate. The specific model layering principle is that all embedding layers are treated as a single layer including position coding, all head layer parameters are treated as a single layer, and the remaining layers are divided according to the construction structure of the model. For example, RoBERTa<sub>base</sub> has 12 hidden layers, thus are divided into 12 layer units. Then we group them according to the divided layers. Table 4 reports hyperparameter used for HiFT.

## B More Experiment Results

Table 5 reports the results of GPT-2 including medium and large on the E2E dataset. We use the same evaluation metrics as Hu et al. (2022a).

<sup>2</sup><https://quoradata.quora.com/First-Quora-Dataset-Release-Question-Pairs>

### B.1 Proportion of Parameters

Figure 4 (a, b, c, d) shows the percentage of memory used by the parameters of each part when fine-tuning LLaMA-2 (7B) under standard FPFT and HiFT with the AdamW optimizer. Figure 4 (e) reports the changes in the amount of peak fine-tuning parameters under HiFT at different model sizes.

### B.2 Results of Memory Profiling

This part of the experiment mainly reports the memory usage of different models fine-tuned with different optimizers. Table 6 and Table 7 report the memory profiling of RoBERTa<sub>base</sub> and RoBERTa<sub>large</sub> fine-tuned on CoLA respectively. Table 8 and Table 9 report the memory profiling of GPT-2<sub>large</sub> and GPT-Neo fine-tuned on E2E respectively.

### B.3 Time Profiling

This part mainly provides the time results of the fine-tuning process of the RoBERTa<sub>base</sub> 10, RoBERTa<sub>large</sub> 10, and OPT-13B 11 models.

### B.4 Prompts

Tables 12 and 13 gives detailed prompts of different datasets.

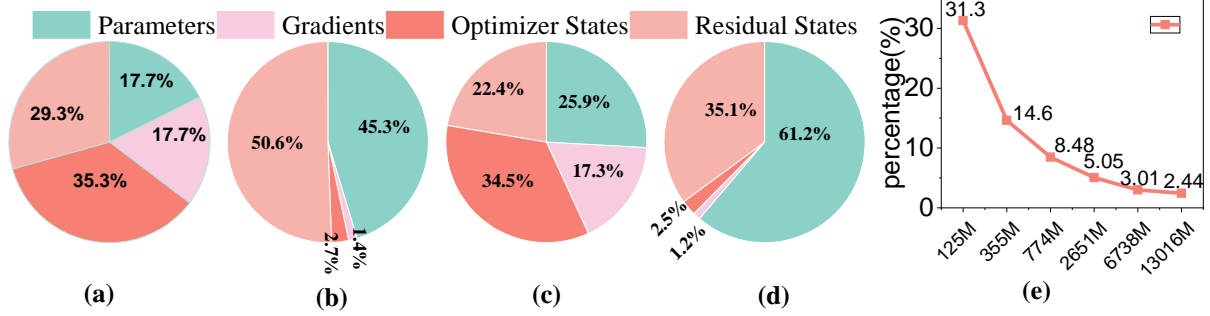


Figure 4: (a), (b), (c) and (d) represent the proportion of parameters occupied by different parts when fine-tuning LLaMA-2 (7B). The sequence length and batch size are set to 512 and 6. (a): 32-bit precision FPFT; (b): 32-bit precision HiFT; (c) mixed precision FPFT; (d): mixed precision HiFT. Fine-tuning uses the AdamW optimizer. The  $m$  is set to 1 for HiFT. (e) represents the change in the proportion of the peak trainable parameters to the total model parameters during the HiFT training under different size models.

Experiment	Hyperparameters	Values
RoBERTa-base	Total Batch size	64
	Learning rate	{ $1e-5$ , $2e-5$ , $3e-5$ }
	warmup	{0.0, 0.02, 0.06}
	Epochs	{50, 100}
	Device	8*GTX 1080Ti (11G)
RoBERTa-large	Total Batch size	32
	Learning rate	{ $1e-5$ , $2e-5$ , $3e-5$ }
	warmup	{0.0, 0.02, 0.06}
	Epochs	{50, 100}
	Device	8*GTX 1080Ti (11G)
GPT-2 (M)	Batch size	32
	Learning rate	{ $5e-5$ }
	warmup	{0.0}
	Epochs	{20}
	Device	RTX A6000 (48G)
	Temperature	0.8
	Beam size	10
	repetition penalty	4
	length penalty	0.9
GPT-2 (L)	Batch size	32
	Learning rate	{ $5e-5$ }
	warmup	{0.0}
	Epochs	{20}
	Device	RTX A6000 (48G)
	Temperature	0.8
	Beam size	10
	repetition penalty	4
	length penalty	0.9
RoBERTa-large	Batch size ( $k = 16$ )	{2, 4, 8}
	Batch size ( $k = 512$ )	{8, 16, 32}
	Learning Rates	{ $1e-5$ , $3e-5$ , $5e-5$ , $8e-5$ }
	Device	8*GTX 1080Ti (11G)
	Weight Decay	0
	Steps ( $k = 16$ )	2,000
Steps ( $k = 512$ )	4,000	
OPT-13B	Batch size	{2, 4, 8}
	Learning Rates	{ $1e-5$ , $2e-5$ , $5e-5$ , $8e-5$ }
	Epochs	5
	Device	A100 (80G)
	Weight Decay	0

Table 4: The hyperparameter grids used for HiFT experiments.



E2E NLG Challenge					
Model & Method	BLUE	NIST	MET	ROUGE-L	CIDEr
GPT-2 M (FPFT) <sup>†</sup>	68.20	8.62	46.20	71.00	2.47
GPT-2 M (Adapter <sup>L</sup> ) <sup>†</sup>	66.30	8.41	45.00	69.80	2.40
GPT-2 M (Adapter <sup>H</sup> ) <sup>†</sup>	67.30	8.50	46.00	70.70	2.44
GPT-2 M (FPFT <sup>Top2</sup> ) <sup>†</sup>	68.10	8.59	46.00	70.80	2.41
GPT-2 M (PreLayer) <sup>†</sup>	69.70	8.81	46.10	71.40	2.49
GPT-2 M (LoRA) <sup>†</sup>	<b>70.40</b>	<b>8.85</b>	<b>46.80</b>	<b>71.80</b>	<b>2.53</b>
HiFT	69.40	8.67	46.77	71.26	2.46
GPT-2 L (FPFT) <sup>†</sup>	68.50	8.78	46.00	69.90	2.45
GPT-2 L (Adapter <sup>L</sup> ) <sup>†</sup>	69.10	8.68	46.30	71.40	<b>2.49</b>
GPT-2 L (PreLayer) <sup>†</sup>	70.30	8.85	46.20	71.70	2.47
GPT-2 L (LoRA) <sup>†</sup>	<b>70.40</b>	<b>8.89</b>	<b>46.80</b>	72.00	2.47
HiFT	70.30	8.86	46.64	<b>72.22</b>	2.48

Table 5: GPT-2 medium (M) and large (L) with different fine-tuning methods on the E2E NLG Challenge. For all metrics, higher is better.  $m$  of HiFT is set to 1. <sup>†</sup> means the result comes from [Hu et al. \(2022a\)](#)

Optimizer	#Dtype	#FType	#Trainable				Residual		
			Parameters	#Para(MB)	#Gra(MB)	#Sta(MB)	#PGS(GB)	States(GB)	Total(GB)
AdamW	fp32	FPFT	124.65M	475.49	475.49	950.98	1.86	5.02	6.88
		HiFT	39.00M	475.49	148.77	297.54	0.90	3.61	4.52
	mixed	FPFT	124.65M	713.25	475.49	950.98	2.09	3.58	5.67
		HiFT	39.00M	713.25	148.77	297.54	1.13	2.58	<b>3.71</b>
SGDM	fp32	FPFT	124.65M	475.49	475.49	475.49	1.39	5.00	6.39
		HiFT	39.00M	475.49	148.77	148.77	0.75	3.76	4.52
	mixed	FPFT	124.65M	713.25	475.49	475.49	1.63	3.57	5.20
		HiFT	39.00M	713.25	148.77	148.77	0.99	2.71	<b>3.69</b>
SGD	fp32	FPFT	124.65M	475.49	475.49	0.00	0.93	4.97	5.90
		HiFT	39.00M	475.49	148.77	0.00	0.61	3.91	4.52
	mixed	FPFT	124.65M	713.25	475.49	0.00	1.16	3.57	4.73
		HiFT	39.00M	713.25	148.77	0.00	0.84	2.88	<b>3.72</b>
Adafactor	fp32	FPFT	124.65M	475.49	475.49	0.98	0.93	4.98	5.91
		HiFT	39.00M	475.49	148.77	0.19	0.61	3.91	4.52
	mixed	FPFT	124.65M	713.25	475.49	0.98	1.16	3.57	4.73
		HiFT	39.00M	713.25	148.77	0.19	0.84	2.87	<b>3.71</b>
Adagrad	fp32	FPFT	124.65M	475.49	475.49	475.49	1.39	5.00	6.39
		HiFT	39.00M	475.49	148.77	148.77	0.75	3.76	4.52
	mixed	FPFT	124.65M	713.25	475.49	475.49	1.63	3.57	5.20
		HiFT	39.00M	713.25	148.77	148.77	0.99	2.71	<b>3.69</b>

Table 6: The GPU memory usage of fine-tuning RoBERTa<sub>base</sub> on the CoLA dataset. The sequence length and batch size are set to 512 and 8, respectively. **#Dtype** represents the data type used for training, where **FP32** represents fully parameter fine-tuning the model with 32-bit precision, and **mixed** represents fine-tuning with mixed precision. **#Trainable parameters** represents the maximum number of trainable parameters that appear in a single step during the fine-tuning process. **#Para** represents the memory occupied by the model parameters, **#Gra** represents the memory occupied by the gradient, and **#Sta** represents the memory occupied by the optimizer state. **#PGS** represents the sum of memory occupied by model parameters (i.e., **#Para**), gradients (i.e., **#Gra**) and optimizer state (i.e., **#Sta**). **Residual states** mainly includes activation, temporary buffers and unusable fragmented memory. **Total** represents the total memory used during fine-tuning. The parameter  $m$  of HiFT is set to 1.

Optimizer	#Dtype	#FType	#Trainable				Residual		
			Parameters	#Para(MB)	#Gra(MB)	#Sta(MB)	#PGS(GB)	States(GB)	Total(GB)
AdamW	fp32	FPFT	355.36M	1355.60	1355.60	2711.20	5.30	13.08	18.38
		HiFT	52.00M	1355.60	198.38	396.73	1.90	9.97	11.88
	mixed	FPFT	355.36M	2033.40	1355.60	2711.20	5.96	9.30	15.25
		HiFT	52.00M	2033.40	198.38	396.73	2.57	7.17	<b>9.74</b>
SGDM	fp32	FPFT	355.36M	1355.60	1355.60	1355.60	3.97	13.08	17.05
		HiFT	52.00M	1355.60	198.38	198.38	1.71	10.20	11.91
	mixed	FPFT	355.36M	2033.40	1355.60	1355.60	4.63	9.30	13.93
		HiFT	52.00M	2033.40	198.38	198.38	2.37	7.36	<b>9.74</b>
SGD	fp32	FPFT	355.36M	1355.60	1355.60	0.00	2.65	13.08	15.73
		HiFT	52.00M	1355.60	198.38	0.00	1.52	10.36	11.88
	mixed	FPFT	355.36M	2033.40	1355.60	0.00	3.31	9.30	12.60
		HiFT	52.00M	2033.40	198.38	0.00	2.18	7.56	<b>9.74</b>
Adafactor	fp32	FPFT	355.36M	1355.60	1355.60	3.14	2.65	13.08	15.73
		HiFT	52.00M	1355.60	198.38	0.21	1.52	10.36	11.88
	mixed	FPFT	355.36M	2033.40	1355.60	3.14	3.31	9.30	12.61
		HiFT	52.00M	2033.40	198.38	0.21	2.18	7.51	<b>9.69</b>
Adagrad	fp32	FPFT	355.36M	1355.60	1355.60	1355.60	3.97	13.08	17.05
		HiFT	52.00M	1355.60	198.38	198.38	1.71	10.20	11.91
	mixed	FPFT	355.36M	2033.40	1355.60	1355.60	4.63	9.30	13.93
		HiFT	52.00M	2033.40	198.38	198.38	2.37	7.36	<b>9.74</b>

Table 7: The GPU memory usage of fine-tuning RoBERTa<sub>large</sub> on the CoLA dataset. The sequence length and batch size are set to 512 and 8, respectively.

Optimizer	#Dtype	#FType	#Trainable				Residual		
			Parameters	#Para(MB)	#Gra(MB)	#Sta(MB)	#PGS(GB)	States(GB)	Total(GB)
AdamW	fp32	FPFT	774.03M	2952.69	2952.69	5905.39	11.53	37.26	48.79
		HiFT	65.64M	2952.69	250.40	500.79	3.62	31.73	35.35
	mixed	FPFT	774.03M	4429.05	2952.69	5905.39	12.98	28.13	41.11
		HiFT	65.64M	4429.05	250.40	500.79	5.06	24.97	<b>30.03</b>
SGDM	fp32	FPFT	774.03M	2952.69	2952.69	2952.69	8.65	37.26	45.91
		HiFT	65.64M	2952.69	250.40	250.40	3.37	31.98	35.35
	mixed	FPFT	774.03M	4429.05	2952.69	2952.69	10.09	28.14	38.23
		HiFT	65.64M	4429.05	250.40	250.40	4.81	25.22	<b>30.03</b>
SGD	fp32	FPFT	774.03M	2952.69	2952.69	0.00	5.77	37.25	43.02
		HiFT	65.64M	2952.69	250.40	0.00	3.13	32.22	35.35
	mixed	FPFT	774.03M	4429.05	2952.69	0.00	7.21	28.12	35.33
		HiFT	65.64M	4429.05	250.40	0.00	4.57	25.46	<b>30.03</b>
Adafactor	fp32	FPFT	774.03M	2952.69	2952.69	5.31	5.77	37.26	43.03
		HiFT	65.64M	2952.69	250.40	0.21	3.13	32.22	35.35
	mixed	FPFT	774.03M	4429.05	2952.69	5.31	7.21	28.12	35.33
		HiFT	65.64M	4429.05	250.40	0.21	4.57	25.46	<b>30.03</b>
Adagrad	fp32	FPFT	774.03M	2952.69	2952.69	2952.69	8.65	37.26	45.91
		HiFT	65.64M	2952.69	250.40	250.40	3.37	31.98	35.35
	mixed	FPFT	774.03M	4429.05	2952.69	2952.69	10.09	28.13	38.22
		HiFT	65.64M	4429.05	250.40	250.40	4.81	25.22	<b>30.03</b>

Table 8: The GPU memory usage of fine-tuning GPT-2<sub>large</sub> on the E2E dataset. The sequence length and batch size are set to 512 and 8, respectively.

Optimizer	#Dtype	#FType	#Trainable				Residual		
			Parameters	#Para(MB)	#Gra(MB)	#Sta(MB)	#PGS(GB)	States(GB)	Total(GB)
AdamW	fp32	FPFT	2651.31M	10113.95	10113.95	20227.89	39.51	22.69	62.20
		HiFT	133.9M	10113.95	510.79	1021.58	11.37	16.95	<b>28.33</b>
	mixed	FPFT	2651.31M	15170.93	10113.95	20227.89	44.45	19.57	64.01
		HiFT	133.9M	15170.93	510.79	1021.58	16.31	15.92	32.23
SGDM	fp32	FPFT	2651.31M	10113.95	10113.95	10113.95	29.63	22.69	52.32
		HiFT	133.9M	10113.95	510.79	510.79	10.87	17.45	<b>28.33</b>
	mixed	FPFT	2651.31M	15170.93	10113.95	10113.95	34.57	19.57	54.13
		HiFT	133.9M	15170.93	510.79	510.79	15.81	16.33	32.14
SGD	fp32	FPFT	2651.31M	10113.95	10113.95	0.00	19.75	22.69	42.44
		HiFT	133.9M	10113.95	510.79	0.00	10.38	17.95	<b>28.33</b>
	mixed	FPFT	2651.31M	15170.93	10113.95	0.00	24.69	19.56	44.26
		HiFT	133.9M	15170.93	510.79	0.00	15.31	16.83	32.14
Adafactor	fp32	FPFT	2651.31M	10113.95	10113.95	8.99	19.76	22.69	42.45
		HiFT	133.9M	10113.95	510.79	0.22	10.38	17.95	<b>28.33</b>
	mixed	FPFT	2651.31M	15170.93	10113.95	8.99	24.70	19.56	44.26
		HiFT	133.9M	15170.93	510.79	0.22	15.31	16.83	32.14
Adagrad	fp32	FPFT	2651.31M	10113.95	10113.95	10113.95	29.63	22.69	52.32
		HiFT	133.9M	10113.95	510.79	510.79	10.87	17.45	<b>28.33</b>
	mixed	FPFT	2651.31M	15170.93	10113.95	10113.95	34.57	19.57	54.14
		HiFT	133.9M	15170.93	510.79	510.79	15.81	16.33	32.14

Table 9: The GPU memory usage of fine-tuning GPT-Neo on the E2E dataset. The sequence length and batch size are set to 512 and 8, respectively.

Models	FTType	SST-2		MNLI		QNLI		QQP		RTE		STS-B		MRPC		CoLA	
		steps/sec	sec/steps	steps/sec	sec/steps	steps/sec	sec/steps	steps/sec	sec/steps	steps/sec	sec/steps	steps/sec	sec/steps	steps/sec	sec/steps	steps/sec	sec/steps
RoBERTa <sub>base</sub>	HiFT	1.42	0.71	1.53	0.70	1.41	0.71	1.40	0.72	1.06	0.94	1.15	0.87	1.12	0.89	1.26	0.79
	FPFT	<b>1.76</b>	<b>0.57</b>	<b>1.78</b>	<b>0.56</b>	<b>1.75</b>	<b>0.57</b>	<b>1.75</b>	<b>0.57</b>	<b>1.10</b>	<b>0.91</b>	<b>1.36</b>	<b>0.73</b>	<b>1.26</b>	<b>0.80</b>	<b>1.48</b>	<b>0.68</b>
RoBERTa <sub>large</sub>	HiFT	<b>1.20</b>	<b>0.83</b>	<b>1.18</b>	<b>0.85</b>	<b>1.18</b>	<b>0.85</b>	<b>1.14</b>	<b>0.88</b>	<b>1.09</b>	<b>0.92</b>	<b>1.05</b>	<b>0.95</b>	<b>1.08</b>	<b>0.93</b>	<b>1.14</b>	<b>0.88</b>
	FPFT	0.86	1.17	0.86	1.16	0.84	1.19	0.84	1.19	0.78	1.28	0.77	1.29	0.79	1.26	0.82	1.22

Table 10: Running time statistics of RoBERTa on different tasks. The steps/sec indicates how many steps are run per second, and sec/steps indicates how long it takes to run each step.

Time	SST2	RTE	CB	BoolQ	WSC	WIC	MultiRC	COPA	ReCoRD	SQuAD	DROP
Sec/steps	8.16	5.47	29.47	5.48	11.55	7.81	5.21	14.46	7.45	4.57	4.13
Total(sec)	5102.21	6841.42	2800.05	6853.32	1022.23	4883.62	6518.04	2747.39	4658.79	5706.37	5166.14

Table 11: Running time statistics of OPT-13B on different tasks. The sec/steps indicates how long it takes to run each step, and total represents the time required to run 5 epochs, including evaluation time.

Dataset	$C$	Type	Prompt	Label words
SST-2	2	sentiment cls.	$\langle S_1 \rangle$ It was [MASK] .	{great, terrible}
SST-5	5	sentiment cls.	$\langle S_1 \rangle$ It was [MASK] .	{great, good, okay, bad, terrible}
TREC	6	topic cls.	[MASK] : $\langle S_1 \rangle$	{Description, Expression, Entity, Human, Location, Number}
MNLI	3	NLI	$\langle S_1 \rangle$ ? [MASK] , $\langle S_2 \rangle$	{Yes, Maybe, No}
SNLI	3	NLI	$\langle S_1 \rangle$ ? [MASK] , $\langle S_2 \rangle$	{Yes, Maybe, No}
RTE	2	NLI	$\langle S_1 \rangle$ ? [MASK] , $\langle S_2 \rangle$	{Yes, No}

Table 12: The prompts of the datasets we used in our RoBERTa-large experiments (i.e., Table 1). The prompts are adapted from (Gao et al., 2021) and include a template and a set of label words that can fill in the [MASK] token.  $\langle S_1 \rangle$  and  $\langle S_2 \rangle$  refer to the first and the second (if any) input sentence.

Dataset	Type	Prompt
SST-2	cls.	$\langle \text{text} \rangle$ It was <b>terrible/great</b>
RTE	cls.	$\langle \text{premise} \rangle$ Does this mean that " $\langle \text{hypothesis} \rangle$ " is true? Yes or No? <b>Yes/No</b>
CB	cls.	Suppose $\langle \text{premise} \rangle$ Can we infer that " $\langle \text{hypothesis} \rangle$ "? Yes, No, or Maybe? <b>Yes/No/Maybe</b>
BoolQ	cls.	$\langle \text{passage} \rangle$ $\langle \text{question} \rangle$ ? <b>Yes/No</b>
WSC	cls.	$\langle \text{text} \rangle$ In the previous sentence, does the pronoun " $\langle \text{span2} \rangle$ " refer to $\langle \text{span1} \rangle$ ? Yes or No? <b>Yes/No</b>
WIC	cls.	Does the word " $\langle \text{word} \rangle$ " have the same meaning in these two sentences? Yes, No? $\langle \text{sent1} \rangle$ $\langle \text{sent2} \rangle$ <b>Yes/No</b>
MultiRC	cls.	$\langle \text{paragraph} \rangle$ Question: $\langle \text{question} \rangle$ I found this answer " $\langle \text{answer} \rangle$ ". Is that correct? Yes or No? <b>Yes/No</b>
COPA	mch.	$\langle \text{premise} \rangle$ so/because $\langle \text{candidate} \rangle$
ReCoRD	mch.	$\langle \text{passage} \rangle$ $\langle \text{query} \rangle$ .replace("@placeholder", $\langle \text{candidate} \rangle$ )
SQuAD	QA	Title: $\langle \text{title} \rangle$ Context: $\langle \text{context} \rangle$ Question: $\langle \text{question} \rangle$ Answer:
DROP	QA	Passage: $\langle \text{context} \rangle$ Question: $\langle \text{question} \rangle$ Answer:

Table 13: The prompts of the datasets we used in our OPT experiments. There are three types of tasks: classification (cls.), multiple-choice (mch.), and question answering (QA).  $\langle \text{text} \rangle$  represents input from the dataset and **Yes** represents label words. For inference on multiple choice tasks, we put in different candidates in the prompt and calculate the average log-likelihood for each candidate, and choose the candidate with the highest score. For inference on QA tasks, we use greedy decoding to generate the answer. All prompts configurations are consistent with Malladi et al. (2023)